Clinical Cancer Research

Development of Immunohistochemistry Assays to Assess GALNT14 and FUT3/6 in Clinical Trials of Dulanermin and Drozitumab

Howard M. Stern[1], Mary Padilla[4], Klaus Wagner[2,5], Lukas Amler[2], and Avi Ashkenazi[3]

Abstract

Purpose: *In vitro* sensitivity to the proapoptotic receptor agonists dulanermin (rhApo2L/TRAIL) and drozitumab (DR5-agonist antibody) is strongly predicted by the expression of the O-glycosylation enzymes GALNT14 in non–small cell lung cancer (NSCLC) cell lines (among others) and of FUT3/6 in colorectal cancer (CRC) cell lines. We developed immunohistochemistry (IHC) assays that measure GALNT14 and FUT3/6 levels in archival formalin-fixed, paraffin-embedded human tumor tissue to determine marker prevalence in NSCLC and CRC tissue and to enable the future examination of these markers in clinical trials.

Experimental Design: GALNT14 or FUT3/6 ELISA-positive hybridoma clones were screened through IHC on cell pellets with known mRNA levels. The specificity of staining was examined in cell lines, normal tissue, and tumor tissue.

Results: GALNT14 and FUT3/6 IHC exhibited a golgi staining pattern and correlated with GALNT14 and FUT3/6 (but not GALNT2 and FUT4) mRNA expression levels in cell lines and normal tissues, suggesting specificity. GALNT14 and FUT3/6 H-scores were significantly higher in cell lines sensitive to dulanermin ($P = 0.01$ and $P = 0.0004$, respectively) and drozitumab ($P = 0.03$ and $P < 0.0001$, respectively) versus resistant cell lines. GALNT14 and FUT3/6 H-scores varied widely, with ~45% of NSCLC samples exhibiting weak to moderate GALNT14 staining (H-score of at least 25) and 70% of CRC samples exhibiting moderate to strong FUT3/6 staining (H-score of at least 125).

Conclusions: GALNT14 and FUT3/6 expression can be assessed in human tumors using sensitive and specific IHC assays. Both assays are being deployed in ongoing clinical trials of dulanermin and drozitumab to assess potential utility for patient selection. *Clin Cancer Res; 16(5); 1587–96. ©2010 AACR.*

Developing oncology drugs that have significant effect for patients has proven to be challenging for many reasons. One contributing factor is the diversity, at the molecular level, of tumors that are classified similarly on the basis of histology. As a consequence, most oncology chemotherapeutics do not impart a clinically meaningful benefit in all treated patients. One strategy for addressing this deficit is the identification of molecular correlates of response (or resistance) to specific therapies to better match drugs with patients who have a high probability of clinical benefit. Accomplishing this task during drug development involves early efforts to identify potential biomarkers in preclinical models and the development of appropriately validated diagnostic assays that can test these biomarkers in early-stage clinical trials.

Agents that target apoptosis are currently the subject of intense investigation and stand to benefit from the development of diagnostic biomarkers. Most cells with cancer-initiating potential are eliminated from the body by apoptosis, but some cells harbor mutations that enable them to escape apoptosis, resulting in cell survival and the development of malignant tumors (2, 3). As our understanding of the molecular basis of apoptosis has increased, so too has research in the development of proapoptotic agents that tip the balance toward tumor cell death. The complex signaling cascade that leads to apoptosis is initiated either intracellularly through the intrinsic pathway or as a result of extracellular signals that trigger the extrinsic pathway (2, 3). Manipulation of the extrinsic pathway has been a major focus of drug discovery. Stimulation of this pathway begins with the binding of a proapoptotic ligand such as apoptosis ligand 2/tumor necrosis factor–related

Authors' Affiliations: Departments of [1]Research Pathology, [2]Development Oncology Diagnostics, and [3]Molecular Oncology, Genentech, Inc., South San Francisco, California; [4]Ventana Medical Systems, Inc., Tucson, Arizona; and [5]M.D. Anderson Cancer Center, Houston, Texas

Note: Supplementary data for this article are available at Clinical Cancer Research Online (http://clincancerres.aacrjournals.org/).

Corresponding Authors: Howard M. Stern, Department of Research Pathology, Genentech, Inc., 1 DNA Way, South San Francisco, CA 94080. Phone: 650-467-8194; Fax: 650-225-8989; E-mail: hstern@gene.com and Avi Ashkenazi, Department of Molecular Oncology, Genentech, Inc., 1 DNA Way, South San Francisco, CA 94080. Phone: 650-225-1853; Fax: 650-467-8195; E-mail: aa@gene.com.

doi: 10.1158/1078-0432.CCR-09-3108

Translational Relevance

The use of predictive diagnostic biomarkers to identify patients who may best respond to a particular type of cancer treatment is emerging as a crucial paradigm in the development of novel cancer therapies. Previous work (1) reported the identification of the O-glycosylation enzymes GALNT14 and FUT3/6 as potential diagnostic biomarkers for predicting response to proapoptotic death receptor agonists. We have developed and validated immunohistochemistry assays to detect GALNT14 and FUT3/6 in human tissue and describe the prevelance of expression in non–small cell lung cancer and colorectal cancer. These assays will enable the examination of GALNT14 and FUT3/6 in clinical trials of proapoptotic death receptor agonists.

apoptosis-inducing ligand to proapoptotic "death receptors" such as DR4 and DR5. Ligand-binding facilitates receptor clustering and the formation of a death-inducing signaling complex through the recruitment of the Fas-associated death domain adaptor protein. Fas-associated death domain helps activate the downstream initiator and effector caspases, which mediate apoptotic cell death (4–8).

Several agents that trigger the extrinsic apoptosis pathway through the activation of the proapoptotic death receptors are currently in development (2, 3). These "proapoptotic receptor agonists" include the recombinant human apoptosis ligand 2 tumor necrosis factor–related apoptosis-inducing ligand (dulanermin), which targets both DR4 and DR5 (2, 3, 9–11), and monoclonal antibodies that activate either DR4 (mapatumumab) or DR5 (drozitumab, lexatumumab, conatumumab, tigatuzumab, and LBY-135; refs. 2, 3, 12–15). Preclinical studies using certain cell lines and *in vivo* xenograft models have shown promising results with these agents in a wide range of tumor types, both alone and in combination with traditional chemotherapies and molecularly targeted agents (2, 16). However, in keeping with most oncology drugs, proapoptotic receptor agonists are not universally effective in all tumor cell lines, resulting in efforts to identify molecular markers that correlate with response.

Recently, Wagner and colleagues (1) showed that sensitivity to dulanermin was strongly correlated with the overexpression of the O-glycosylation initiator enzyme N-acetylgalactosaminyltransferase-14 (GALNT14) in cell lines from several tumor types. Furthermore, in colorectal cancer (CRC) cell lines, dulanermin sensitivity was correlated with the O-glycosylation initiator enzyme, N-acetylgalactosaminyl-transferase-3 (GALNT3), and the fucosyltransferase (FUT) enzymes, FUT3 and FUT6 (1). For reviews on O-glycosylation, see Ten Hagen et al. and Hang and Bertozzi (17, 18). The expression of GALNT14 correlated with dulanermin sensitivity in pancreatic cancer, non–small cell lung cancer (NSCLC), and melanoma cell lines, with up to 30% of tissue samples from a variety of human cancers having relative GALNT14 mRNA expression at levels comparable with those seen in dulanermin-sensitive cell lines (1). In CRC cell lines, GALNT3 rather than GALNT14 mRNA levels were correlated with sensitivity ($P = 0.026$), as were levels of FUT3 and FUT6 mRNA. In fact, high FUT3 and FUT6 levels were better predictors of sensitivity than was GALNT3 ($P = 0.01$ for FUT3 and $P = 0.0013$ for FUT6). Notably, FUT3 and FUT6 mRNA expression levels were highly correlated with each other in these cell lines, suggesting that regulation of expression of these genes is coordinated. Overall, the high expression of GALNT14, GALNT3, FUT3, and FUT6 could predict responsiveness to dulanermin in 61% of cell lines (positive predictive value) and a lack of sensitivity in 88% of cell lines (negative predictive value; ref. 1).

Wagner et al. (1) also showed a functional link between death receptor O-glycosylation and apoptotic signaling. Both pharmacologic inhibition of glycosylation and enzyme knockdown through small interfering RNAs targeting GALNT14-, GALNT3-, and FUT6 reduced dulanermin-induced apoptosis. Furthermore, GALNT14 overexpression in pancreatic cancer cells substantially increased death-inducing signaling complex formation and caspase-8 and caspase-3 processing, whereas the progressive mutation of DR5 at sites of O-glycosylation weakened apoptotic signaling. In addition, GALNT14 knockdown in pancreatic cancer cells and FUT6 knockdown in colon cancer cells reduced caspase-8 processing, but did not appreciably alter DR4 or DR5 levels (1), supporting the conclusion that the glycosylation status of DR4/5 can affect apoptotic signaling independent from DR4/5 levels. Biochemical analysis further revealed that O-glycosylation facilitates ligand-induced clustering of DR4 and DR5, an event required for the efficient recruitment and activation of caspase-8 (1).

More recently, this body of work has been expanded to the examination of sensitivity to the DR5-agonist antibody, drozitumab. As observed for dulanermin, drozitumab sensitivity correlates with the expression of GALNT3, GALNT14, and FUT3/6 expression in several tumor cell types (19). In pancreatic cancer and NSCLC cell lines, statistically significant correlations were observed between GALNT14 levels and drozitumab sensitivity ($P = 0.00029$), whereas in CRC, GALNT3 and FUT3/6 levels were correlated with drozitumab sensitivity, with FUT6 being most strongly predictive ($P = 0.00013$; ref. 19).

Taken together, the results of the Wagner and Punnoose studies indicate, among other things, that GALNT14 levels may be a predictive biomarker for dulanermin- and drozitumab-based therapy in NSCLC (among other indications), whereas FUT3/6 may be a predictive biomarker in CRC. To further test these findings in clinical trials, we developed immunohistochemistry (IHC) assays to measure protein levels of these enzymes in formalin-fixed, paraffin-embedded (FFPE) cancer tissues. The results of the assay validation are presented in this report, as

well as the findings on the distribution of GALNT14 and FUT3/6 in NSCLC and CRC tumors.

Materials and Methods

Antigen and antibody production and screening. cDNAs coding for amino acids 40 to 552 of GALNT14 and 46 to 359 of FUT6 were cloned into a pRK expression vector with the addition of an NH_2-terminal His tag for GALNT14 and an NH_2-terminal Flag tag for FUT6. The vectors were subsequently transfected into Chinese hamster ovary cells for protein production, and the tagged proteins were purified by affinity chromatography using nickel or anti-Flag antibody columns.

Recombinant His-tagged GALNT14 and Flag-tagged FUT6 were denatured in a 0.5% SDS solution at 80°C for 20 min. Female BALB/c mice were hyperimmunized, through the footpad, twice weekly for a total of 12 to 13 boosts with 2 μg/animal denatured antigen resuspended in monophosphoryl lipid A/trehalose dicorynomycolate–based adjuvant (Corixa Corp.). Three days after the final boost, popliteal lymph node cells were extracted and fused with cells derived from the murine myeloma cell line P3X63AgU.1 (ATCC CRL1597; American Type Culture Collection) using 50% polyethylene glycol or electrofusion (CytoPulse Sciences, Inc.). Hybridoma cells were selected using hypoxanthine-aminopterin-thymidine–based media (ClonaCell Medium D, StemCell Technologies). Ten to 14 d postfusion, culture supernatants were collected and screened by direct ELISA for specific binding to denatured His-GALNT14 or Flag-FUT6 versus a SDS-denatured His-tagged or Flag-tagged control protein. For FUT6, an additional ELISA screen determined specific binding to denatured Flag-FUT3.

After the initial screen by ELISA, supernatants were screened through IHC on a tissue microarray constructed from FFPE cell pellets that were known to have high or low mRNA expression of the antigens. IHC-positive cell lines were subcloned two to four times by limiting dilution, and those showing strongest reactivity by ELISA and IHC were scaled up in CELLine Bioreactor Flasks (CL1000, Argos Technologies) for the *in vitro* production of monoclonal antibodies. Bioreactor-generated supernatant was purified by Protein A affinity chromatography, and purified antibody preparations were sterile filtered (0.2-mm pore size; Nalgene) and stored at 4°C in PBS.

IHC protocols. Prototype IHC assay protocols for GALNT14 and FUT3/6 were developed on the BenchMark XT automated staining platform (Ventana Medical Systems, Inc.) using *ultraView* Universal HRP Multimer (Ventana Medical Systems, Inc.) as the secondary antibody, *ultraView* Universal DAB (Ventana Medical Systems, Inc.) for the detection system, and Hematoxylin II (Ventana Medical Systems, Inc.) for the counter stain.

The antigen retrieval conditions were tested as follows: no pretreatment, mild Cell Conditioning 1 (Ventana Medical Systems, Inc.; 30 min, 100°C; pH 8), standard Cell Conditioning 1 (60 min, 100°C; pH 8), and mild Cell Conditioning 2 (30 min, 100°C; pH 6) using FFPE normal kidney tissue for GALNT14 and normal colon for FUT3/6. In both cases, standard Cell Conditioning 1 achieved the best staining characteristics, with a primary antibody incubation time of 16 min and temperature of 37°C. For GALNT14, two clones (5C4 and 3F11) were titered on FFPE normal kidney tissue, NSCLC tissues, and NSCLC cell pellets. 3F11 was the more sensitive antibody and was chosen for the final assay with a dilution of 1.6 μg/mL. For FUT3/6, the 1G11 clone was titered on FFPE normal colon, CRC, and CRC cell pellets, and a 1.3 μg/mL dilution chosen. The final dilution for both assays maximized signal-to-noise ratio across the tissues and cell lines tested. Five primary antibody diluents were tested, and Ventana Tris-HCl primary antibody diluent (Ventana Medical Systems, Inc.) was found to be optimal.

ELISA screening. To screen hybridoma cell supernatant, ELISA was done as previously described (32). Briefly, 96- or 384-well plates were coated with 50 to 100 μL of denatured, tagged antigen or denatured, tagged control protein at 1 μg/mL in coating buffer [0.05 mol/L carbonate buffer (pH 9.6)], sealed, and stored overnight at 4°C. After removing the coating solution, 200 μL (100 μL for a 384-well plate) of assay/blocking solution containing 0.5% bovine serum albumin and 0.05% Tween 20 in PBS (pH 7.4; ELISA diluent) was added to each well, and plates were incubated at room temperature for 1 h with agitation. Wells were then washed thrice with 300 μL (or 120 μL for a 384-well plate) 0.05% Tween 20 in PBS (wash buffer).

After the washing step, 100 μL (50 μL for a 384-well plate) of supernatant from each individual hybridoma clone was added to each well containing denatured, tagged antigen or denatured, tagged control protein. Plates were incubated at room temperature for 1 h with agitation, and the wells were washed thrice with wash buffer as before. After washing, 100 μL (50 μL for a 384-well plate) of a 1:1,000 dilution of peroxidase-conjugated goat IgG fraction to mouse IgG Fc (MP Biomedicals) in ELISA diluent was added to each well. Plates were incubated at room temperature for 1 h with agitation, washed thrice with wash buffer as before, and patted dry. Wells were developed by adding 100 μL (50 μL for a 384-well plate) of the tetramethylbenzidine microwell peroxidase substrate (BioFX Laboratories) to each well and incubating at room temperature for 5 to 10 min or until a good color change was observed. Development was stopped by adding 100 μL (50 μL for a 384-well plate) of the tetramethylbenzidine Stop Solution (BioFX Laboratories) to each well. Plates were analyzed with a Sunrise plate reader (Tecan US, Inc.) at 650 nm. Prebleed and polysera were used as controls. Prebleed samples contained mouse sera before immunization, and polysera samples contained mouse anti-sera obtained after 7 to 10 immunizations.

Cell lines. Panels of NSCLC and CRC cell lines were obtained from the American Type Culture Collection (authenticates through genomic and phenotypic approaches) or the German Collection of Microorganisms and Cell Cultures (authenticates through DNA typing,

cytogenetic and immunophenotypic tests) and passaged for <6 mo after resuscitation. Cell lines were treated with dulanermin or drozitumab to determine responsiveness as previously described (1, 19). The same cell lines were subjected to Affymetrix (Affymetrix, Inc.) mRNA expression profiling (1) and were processed into FFPE cell pellets for IHC. The following NSCLC cell lines were used in this study: A427, A549, CALU-1, EKVX, H1299, H1435, H1568, H1650, H1666, H1703, H1793, H1838, H1975, H2009, H2030, H2122, H2126, H226, H23, H2405, H292, H322T, H358, H441, H460, H520, H522, H596, H647, H650, H661, HOP-18, HOP-62, HOP92, LXFL-529, NCI-1781, NCI-H1155, NCI-H1651, NCI-H838, SK-MES, and SW1573. The following CRC cell lines were used in this study: C170, CACO-2, CL11, CL-34, COLO 201, Colo205, Colo206-F, Colo320 HSR, Colo320-DM, Colo678, Colo741, CX-1, DLD-1, HCT 8, HCT-116, HCT15, HT29, HT55, KM12, LoVo, LS1034, LS180, RKO-A545.1, RKO, SK-CO-1, SW 1417, SW116, SW403, SW480, SW620, SW837, and SW948. The mRNA expression of the various GALNT and FUT family genes was determined from previously described data sets available through GeneLogic (normal tissues) or through Affymetrix-based gene profiling (cell lines; ref. 1). The Affymetrix gene probes (Affymetrix, Inc.) used were as follows: GALNT14- 219271_at, GALNT2- 217788_s_at, FUT3-214088_s_at, FUT6-211465_x_at, FUT4-209892_at, FUT5-211225_at, and FUT7-210506_at.

FFPE cell pellets were produced by growing eight T175 flasks for each cell line, dislodging cells with 10 mmol/L EDTA (pH 8.0) followed by centrifugation, washing in PBS, and then fixation overnight in 10% neutral buffered formalin. Fixed pellets were processed in a Tissue-Tek processor (Sakura Finetek USA) and then embedded in a paraffin block.

Tissues. Normal tissues (including, lung, kidney, colon, and prostate) and cancer tissues (including CRC and NSCLC) were obtained from commercial vendors, without any personal identifiers and without any clinical outcome information. Tissue microarrays were created from cell pellet blocks or tissue blocks with a tissue arrayer (Beecher Instruments) using duplicate or triplicate 0.6-mm cores.

Scoring of IHC staining. For GALNT14 and FUT3/6, data from cell lines and tissues were collected as H-score components based on the H-score approach initiated by McCarty and colleagues (20). The percentage of tumor cells with no staining (0), weak staining (1+), moderate staining (2+), and strong staining (3+) was recorded for each sample. This information was summarized into a single H-score that was the sum of the percent with a score of 1+, twice the percent 2+, and thrice the percent 3+.

Results

GALNT14 IHC assay validation in NSCLC. Mouse monoclonal antibodies to GALNT14 were produced by immunizing mice with GALNT14 protein (amino acids 40-552), screening hybridomas through ELISA, and then screening ELISA-positive clones through IHC on FFPE cell pellets known to have high or low endogenous levels of GALNT14 mRNA. Because of its role in glycosylation, GALNT14 was expected to be expressed in a punctate perinuclear pattern consistent with the Golgi apparatus (21). Two hybridoma supernatants (5C4 and 3F11) resulted in the expected IHC staining pattern and were selected for subcloning and further assay development. Using affinity-purified antibody, both 5C4 and 3F11 were tested on the Ventana BenchMark XT platform using several NSCLC cell lines and human tumors. 3F11 was the more sensitive antibody and was chosen for further characterization at an optimized dilution of 1.6 μg/mL as described in Materials and Methods.

The specificity of the IHC staining pattern was first examined by performing IHC on a tissue microarray containing a panel of 41 FFPE NSCLC cell pellets for which the mRNA expression status of GALNT14 was known. As an example, H1435 is a cell line with relatively low GALNT14 mRNA expression, and there was no evidence of staining in the same cell line through GALNT14 IHC (Fig. 1A). In contrast, HOP18 exhibits relatively high GALNT14 mRNA expression and is strongly positive by GALNT14 IHC (Fig. 1B). To enable a comparison of mRNA levels versus IHC staining across the panel of NSCLC cell lines, IHC staining intensity and proportion of positive cells was captured for each of the cell lines and then condensed into an H-score (20). The mRNA expression, as determined by the Affymetrix gene expression profiling, correlated with H-scores for GALNT14 IHC with

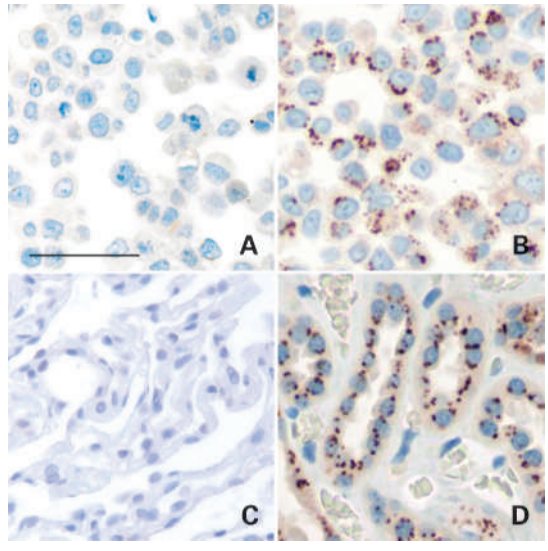

Fig. 1. Examples of GALNT14 IHC. Immunohistochemical staining patterns in cell lines and normal tissues known to express this enzyme (B and D) and known to lack this enzyme (A and C). A, H1435 NSCLC cell line; B, HOP18 NSCLC cell line; C, normal lung tissue; D, normal renal tubules. Scale bar, 50 μm.

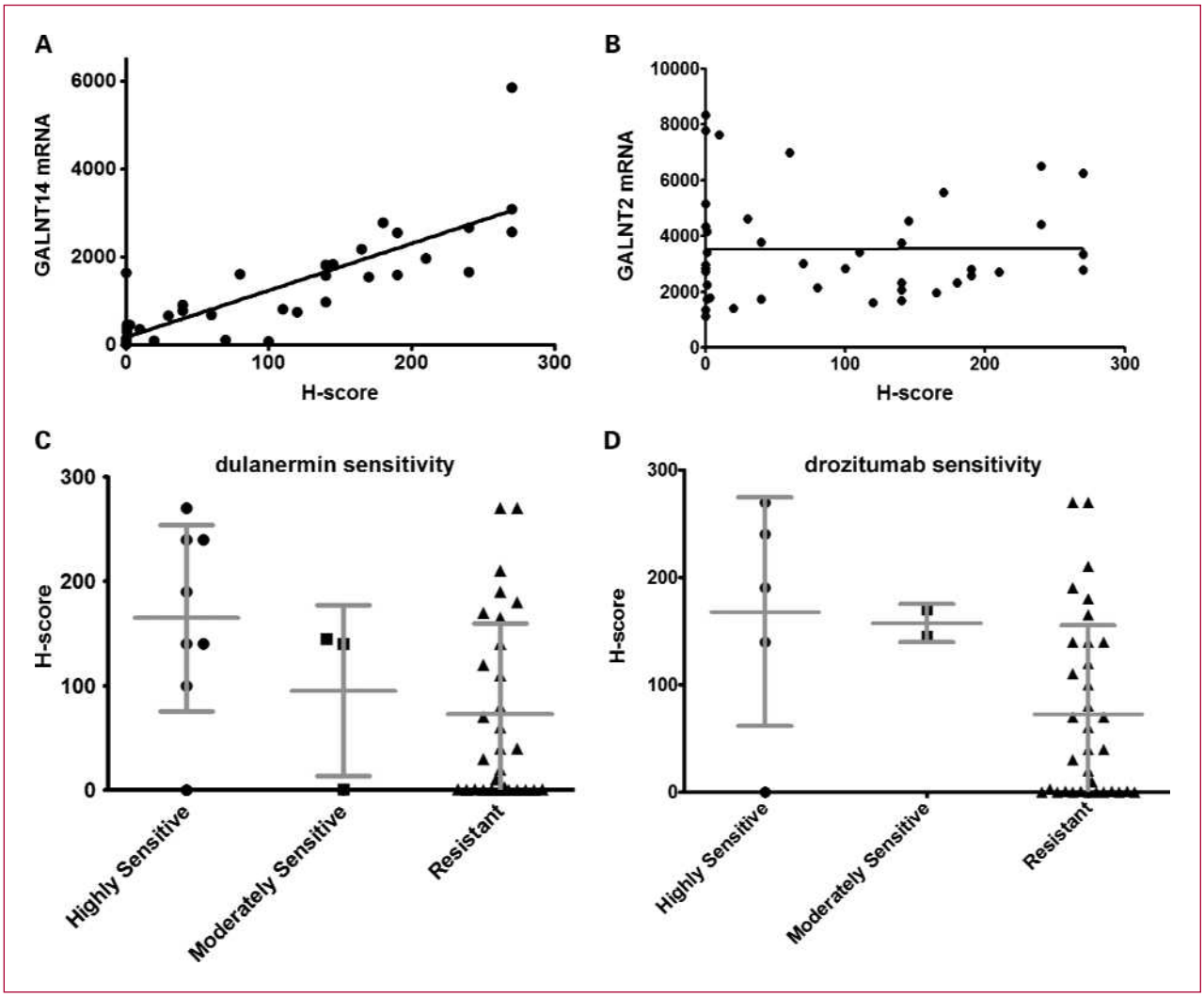

Fig. 2. GALNT14 assay validation. Correlation of GALNT14 IHC H-scores with (A) GALNT14 mRNA levels (r^2 = 0.70) and (B) GALNT2 mRNA levels (r^2 = 0.00003) in 41 NSCLC cell lines. mRNA values are expressed as Affymetrix MAS 5.0 intensity scaled to a trimmed mean of 500. GALNT14 IHC H-scores in cell lines with known sensitivity or resistance to (C) dulanermin (P = 0.01 for highly sensitive versus resistant) and (D) drozitumab (P = 0.03 for highly sensitive versus resistant); points, mean; bars, SD.

a correlation coefficient of 0.70 (Fig. 2A). There was no evidence of correlation between GALNT14 IHC H-score and mRNA expression of the most closely related GALNT family member, GALNT2 (Fig. 2B), which is 50% identical and 67% similar to GALNT14 at the amino acid level (22), suggesting specificity for GALNT14.

The same cell lines had been previously grouped into those that are highly sensitive, moderately sensitive, or resistant to dulanermin and drozitumab (1, 19). GALNT14 IHC H-scores were significantly higher in the highly sensitive cell lines than in resistant cell lines for both dulanermin (P = 0.01) and drozitumab (P = 0.03; Fig. 2C and D).

As a next step in evaluating specificity, we used a database of the Affymetrix gene expression profiling on normal human tissues (GeneLogic) to identify tissues that were relatively high or low in expression of GALNT14 and its most closely related family member, GALNT2. GALNT14 expression is high in normal kidney tissue and low in normal lung tissue (Supplementary Fig. S1). By GALNT14 IHC, punctate perinuclear staining was observed in renal tubules, and no expression was observed in normal lung tissue (Fig. 1C and D), consistent with mRNA expression. By contrast, GALNT2 mRNA expression is equivalent and relatively low in kidney and lung tissue (Supplementary Fig. S1). Together, these data support the conclusion that the GALNT14 IHC assay exhibits evidence of specificity.

The GALNT14 IHC protocol validated on cell lines and normal tissue was then applied to a tissue microarray representing 67 archival NSCLC specimens. Again, the percentage of tumor cells with no staining (0), weak staining intensity (1+), moderate staining intensity (2+), and strong staining intensity (3+) was recorded and then

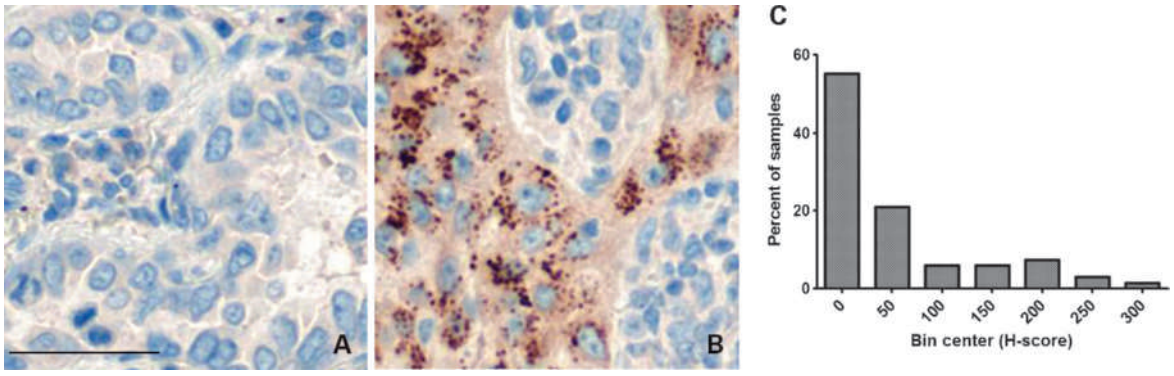

Fig. 3. A wide spectrum of GALNT14 staining patterns is observed in NSCLC tissue ranging from no staining (A) to strongly positive (B). In all cases, dark-brown positive staining is noted in a punctate perinuclear pattern. C, GALNT14 staining in a panel of archival human NSCLC tumors. The frequency distribution is summarized by H-score. Scale bar, 50 μm

condensed into an H-score (20). Examples of samples with no staining and strong staining are illustrated in Fig. 3A and B, respectively. The frequency distribution of GALNT14 staining by H-score for all the samples is summarized in Fig. 3C. Using this scoring system, it is apparent that there is a broad range of staining in NSCLC, with 45% of samples having weak to moderate staining (arbitrarily defined as an H-score of >25).

FUT3/6 IHC assay validation in CRC. Mouse monoclonal antibodies to FUT6 were produced by immunizing mice with the FUT6 protein (amino acids 46-359), and then screening clones by ELISA and IHC on FFPE cell

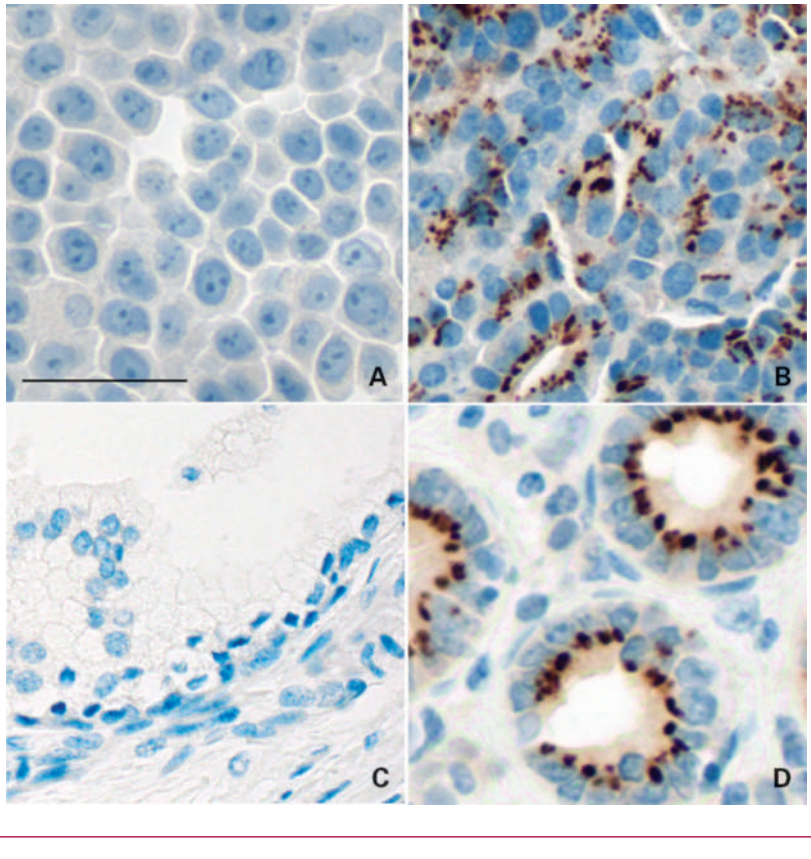

Fig. 4. Examples of FUT3/6 IHC. Immunohistochemical staining patterns in cell lines and normal tissues known to express this enzyme (B and D) and known to lack this enzyme (A and C). Dark-brown positive staining is noted in a punctate perinuclear pattern consistent with the Golgi. A, HT29 CRC cell line; B, SW403 CRC cell line; C, normal prostate tissue; D, normal colon tissue. Scale bar, 50 μm.

pellets similar to the approach with GALNT14. It should be noted that FUT3 and FUT6 are highly homologous (84% identical and 90% similar based on amino acid sequence). Not surprisingly, most hybridomas cross-reacted with both antigens in an ELISA format. Whether the antibody chosen was specific for FUT6 over FUT3 was not considered to be critical because FUT3 and FUT6 expression are highly correlated (1), and both predict response to dulanermin equally well in CRC cell lines (1). The clone 1G11, which cross-reacts with FUT3 and FUT6 by ELISA, resulted in the expected punctate perinuclear IHC staining pattern characteristic of the Golgi apparatus in positive control cell pellets and was selected for further development on the Ventana BenchMark XT platform. An optimized IHC protocol was developed with a final primary antibody dilution of 1.3 μg/mL as described in Materials and Methods.

FUT3/6 IHC was examined in a panel of 32 CRC cell lines and was scored using the H-score (20). Some cell lines, such as HT29, exhibited no staining at all, and other cell lines, such as SW403, exhibited strong, punctate perinuclear staining (Fig. 4A and B). The IHC staining summarized by H-score was examined in relation to the mRNA expression of both FUT3 and FUT6 across the panel of cell lines. In both cases, IHC staining correlated with mRNA expression for FUT3 (r^2 = 0.55) and FUT6 (r^2 = 0.45; Fig. 5A and B). To address specificity, we turned to the three FUT family members most closely related at the protein level: FUT5 (85% identical, 88% similar), FUT7 (47% identical, 63% similar), and FUT4 (43% identical, 56% similar; ref. 23). Of these, only FUT4 is expressed in CRC (Supplementary Fig. S2A), the tumor type in which FUT3/6 is believed to predict response to dulanermin or drozitumab. Consequently, the correlation

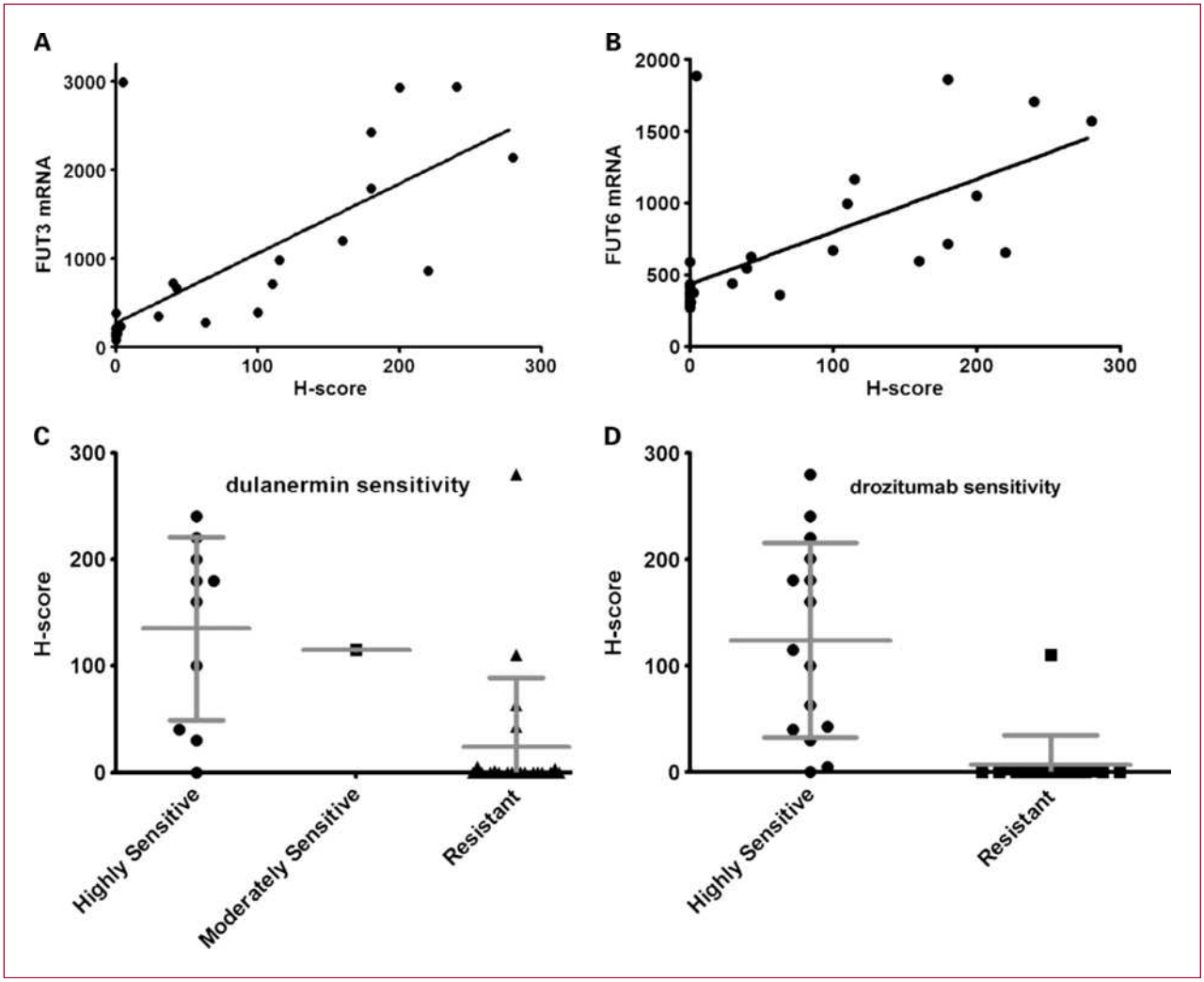

Fig. 5. FUT3/6 assay validation. Correlation of FUT3/6 IHC H-scores with (A) FUT3 mRNA levels (r^2 = 0.55) and (B) FUT6 mRNA levels (r^2 = 0.45) in 32 CRC cell lines. mRNA values expressed as Affymetrix MAS 5.0 intensity scaled to a trimmed mean of 500. FUT3/6 IHC H-scores in cell lines with known sensitivity or resistance to (C) dulanermin (P = 0.0004 for highly sensitive compared with resistant) and (D) drozitumab (P < 0.0001 for highly sensitive compared with resistant); points, mean; bars, SD.

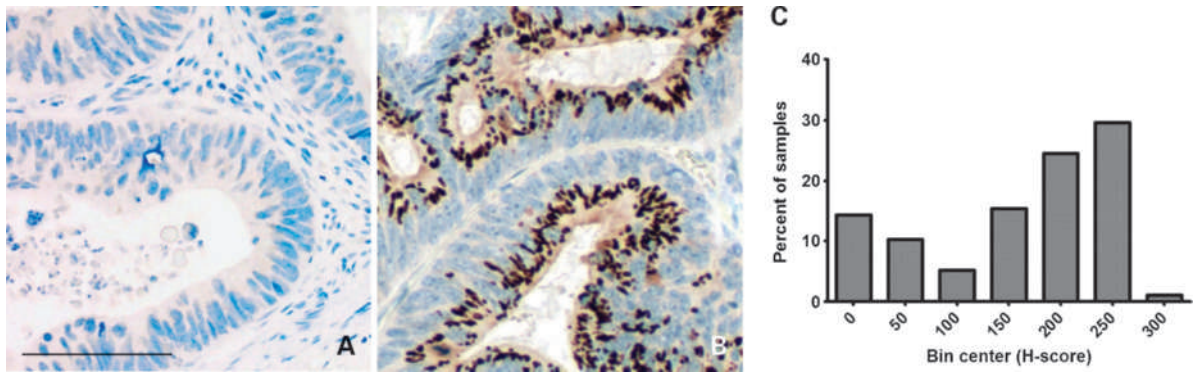

Fig. 6. A wide spectrum of FUT3/6 staining patterns is observed in CRC tissue ranging from no staining (A) to strongly positive (B). In all cases, dark-brown positive staining is noted in a punctate perinuclear pattern. C, FUT3/6 staining in a panel of 98 archival human CRC tumors. The frequency distribution is summarized by H-score. Scale bar, 50 μm.

between FUT3/6 IHC and FUT4 mRNA expression was examined in CRC cell lines. No evidence of correlation was found (Supplementary Fig. S2B), suggesting that the FUT3/6 IHC exhibits some level of specificity.

We next used the CRC cell lines to examine the correlation of FUT3/6 IHC H-scores with *in vitro* sensitivity to dulanermin and drozitumab. There was a very clear, statistically significant relationship between high FUT3/6 IHC staining and cell lines that were highly sensitive versus those that were resistant ($P = 0.0004$ for dulanermin and $P < 0.0001$ for drozitumab; Fig. 5C and D).

As a next step in evaluating specificity, FUT3 and FUT6 mRNA expression was examined in normal human tissues. Normal colon tissue was found to have relatively high expression for both, whereas normal prostate had relatively low expression for both (Supplementary Fig. S3). The FUT3/6 IHC staining was clearly positive in normal colonic epithelial cells, with the staining located on the luminal side of the nucleus consistent with the location of the Golgi; no staining was observed in normal prostate tissue (Fig. 4C and D), consistent with the known mRNA expression data.

Using the IHC protocol that was validated on cell lines and normal tissues, FUT3/6 was examined in a panel of 98 FFPE CRC tumors represented on two tissue microarrays. As with GALNT14, there was a range of FUT3/6 IHC staining from none (Fig. 6A) to uniform strong staining (Fig. 6B). All CRC samples were scored and summarized using H-scores (20). It is clear that there is a wide range of FUT3/6 staining intensity, with a relatively large percentage of CRC tumors (~70%) exhibiting moderate to strong staining (defined arbitrarily as H-score of >125, Fig. 6C).

Discussion

Recent studies have shown that the response to dulanermin and drozitumab in cell lines and xenograft models correlates with levels of the O-glycosylation enzymes GALNT14—in NSCLC, pancreatic cancer, malignant melanoma, and sarcoma—and FUT3/6 in CRC (1, 19). These findings in preclinical models suggest that these enzymes may be clinically useful biomarkers that predict which patients are more likely to derive benefit from dulanermin and drozitumab. Testing these findings in early-phase clinical trials involves the development of robust assays to measure levels of these enzymes in archival FFPE tumor samples. The current study shows that IHC can be used to assess GALNT14 and FUT3/6 in NSCLC and CRC tissue samples. The protocols developed for GALNT14 and FUT3/6 resulted in robust staining, with the punctate perinuclear pattern consistent with the localization in the Golgi. Based on a comparison with gene expression derived from a panel of cell lines and normal human tissues, there is evidence to suggest that these assays are specific for the targets in question.

In the present study, GALNT14 staining varied widely in human NSCLC tissue, with 45% of the samples having weak to moderate staining. FUT3/6 staining varied in CRC tissue, although a much larger proportion of samples having moderate to strong positive staining (70%). It should be noted that the scoring system used in the current study was chosen as a convenient way to summarize data, and is not meant to communicate potential cutoffs that might distinguish responders from nonresponders. Both markers will be examined in an exploratory manner in ongoing phase II trials of both dulanermin and drozitumab to determine whether there are simple cutoffs that distinguish responders from nonresponders.

Oncology diagnostics currently use a range of techniques to assess the molecular characteristics of tumor tissue, including IHC, fluorescent *in situ* hybridization, and quantitative real-time PCR. IHC methods have several advantages including the capability to measure biomarker expression in small numbers of tumor cells among a large normal cell population, being already

established as a diagnostic technique that is widely used in hospital laboratories, and the ability to be performed in a rapid and cost effective manner (24). IHC does have its challenges, however. It is generally considered to be qualitative rather than quantitative (25) and, when used for patient selection such as with human epidermal growth factor receptor 2, can under some conditions be subject to relatively high false-positive rates (refs. 26–30; resulting in treatment of patients who are unlikely to respond) as well as high false-negative rates (leading to exclusion of patients who may benefit from the treatment; ref. 29). The development of testing accreditation guidelines for companion diagnostics, such as those developed by the American Society of Clinical Oncology and the College of American Pathologists for human epidermal growth factor receptor 2 testing in breast cancer (31), may help reduce discordant testing results not only for existing predictive diagnostic assays but also for those that may emerge in the future.

Differences in GALNT14 and FUT3/6 expression do not seem to be associated with alterations in gene copy number (1); consequently, fluorescent *in situ* hybridization is not appropriate for diagnostic identification of patients with overexpression of these enzymes. quantitative real-time PCR may be an alternative method for measuring GALNT14 and FUT3/6, and may be more quantitative than IHC; however, it may be subject to potential dilution by normal cells, given the need to homogenize tissue rather than observe a signal specifically in tumor cells. Future experiments will address whether quantitative real-time PCR analysis of the O-glycosylation enzymes studied here, compared with IHC, has greater value in this clinical setting.

In conclusion, the IHC protocols developed in this study provide a robust, specific method of assessing the O-glycosylation enzymes, GALNT14 and FUT3/6, in archival FFPE human tissues. Both assays are currently being deployed in phase II clinical trials of dulanermin and drozitumab to further evaluate incorporating IHC analysis of specific O-glycosylation enzymes as a diagnostic component of future clinical development.

Disclosure of Potential Conflicts of Interest

H.M. Stern, L. Amler, and A. Ashkenazi: employees of Genentech, shareholders of Roche; K. Wagner: consultant, Genentech; M. Padilla: employee, Ventana Medical Systems, Inc.

Acknowledgments

We thank Patti Tobin, Ling Huw, Terrence Wong, Theresa Shek, and the Department of Protein Chemistry at Genentech for technical assistance.

The costs of publication of this article were defrayed in part by the payment of page charges. This article must therefore be hereby marked *advertisement* in accordance with 18 U.S.C. Section 1734 solely to indicate this fact.

Received 11/24/2009; accepted 12/29/2009; published OnlineFirst 02/23/2010.

References

1. Wagner KW, Punnoose EA, Januario T, et al. Death-receptor O-glycosylation controls tumor-cell sensitivity to the proapoptotic ligand Apo2L/TRAIL. Nat Med 2007;13:1070–7.
2. Ashkenazi A. Targeting the extrinsic apoptosis pathway in cancer. Cytokine Growth Factor Rev 2008;19:325–31.
3. Ashkenazi A, Herbst RS. To kill a tumor cell: the potential of pro-apoptotic receptor agonists. J Clin Invest 2008;118:1979–90.
4. Ashkenazi A, Dixit VM. Death receptors: signaling and modulation. Science 1998;281:1305–8.
5. Boatright KM, Renatus M, Scott FL, et al. A unified model for apical caspase activation. Mol Cell 2003;11:529–41.
6. Fan TJ, Han LH, Cong RS, Liang J. Caspase family proteases and apoptosis. Acta Biochim Biophys Sin (Shanghai) 2005;37:719–27.
7. Lavrik IN, Golks A, Krammer PH. Caspases: pharmacological manipulation of cell death. J Clin Invest 2005;115:2665–72.
8. Thornberry NA. Caspases: a decade of death research. Cell Death Differ 1999;6:1023–7.
9. Ashkenazi A. Targeting death and decoy receptors of the tumour-necrosis factor superfamily. Nat Rev Cancer 2002;2:420–30.
10. Ashkenazi A, Pai RC, Fong S, et al. Safety and antitumor activity of recombinant soluble Apo2 ligand. J Clin Invest 1999;104:155–62.
11. Kelley SK, Ashkenazi A. Targeting death receptors in cancer with Apo2L/TRAIL. Curr Opin Pharmacol 2004;4:333–9.
12. Adams C, Totpal K, Lawrence D, et al. Structural and functional analysis of the interaction between the agonistic monoclonal antibody Apomab and the proapoptotic receptor DR5. Cell Death Differ 2008;15:751–61.
13. Marini P. Drug evaluation: lexatumumab, an intravenous human agonistic mAb targeting TRAIL receptor 2. Curr Opin Mol Ther 2006;8:539–46.
14. Vulfovich M, Saba N. Technology evaluation: mapatumumab, Human Genome Sciences/GlaxoSmithKline/Takeda. Curr Opin Mol Ther 2005;7:502–10.
15. Yada A, Yazawa M, Ishida S, et al. A novel humanized anti-human death receptor 5 antibody CS-1008 induces apoptosis in tumor cells without toxicity in hepatocytes. Ann Oncol 2008;19:1060–7.
16. Ashkenazi A, Holland P, Eckhardt SG. Ligand-based targeting of apoptosis in cancer: the potential of recombinant human apoptosis ligand 2/Tumor necrosis factor-related apoptosis-inducing ligand (rhApo2L/TRAIL). J Clin Oncol 2008;26:3621–30.
17. Hang HC, Bertozzi CR. The chemistry and biology of mucin-type O-linked glycosylation. Bioorg Med Chem 2005;13:5021–34.
18. Ten Hagen KG, Fritz TA, Tabak LA. All in the family: the UDP-GalNAc:polypeptide N-acetylgalactosaminyltransferases. Glycobiology 2003;13:1R–16R.
19. Punnoose EA, Wagner KW, Amler L, Ashkenazi A. Sensitivity to Apomab, an agonistic DR5 specific antibody, is correlated with expression of specific O-glycosyl transferases in tumor-cell lines of both epithelial and non epithelial origin [abstract]. Proceedings of the 100th Annual Meeting of the American Association for Cancer Research 2009, San Diego, CA. Abstract #687.
20. McCarty KS, Jr., Miller LS, Cox EB, Konrath J, McCarty KS Sr. Estrogen receptor analyses. Correlation of biochemical and immunohistochemical methods using monoclonal antireceptor antibodies. Arch Pathol Lab Med 1985;109:716–21.
21. Lowe JB. Glycan-dependent leukocyte adhesion and recruitment in inflammation. Curr Opin Cell Biol 2003;15:531–8.
22. Wang H, Tachibana K, Zhang Y, et al. Cloning and characterization of a novel UDP-GalNAc:polypeptide N-acetylgalactosaminyltransferase, pp-GalNAc-T14. Biochem Biophys Res Commun 2003;300:738–44.
23. Oriol R, Mollicone R, Cailleau A, Balanzino L, Breton C. Divergent

evolution of fucosyltransferase genes from vertebrates, invertebrates, and bacteria. Glycobiology 1999;9:323–34.
24. Papadopoulos N, Kinzler KW, Vogelstein B. The role of companion diagnostics in the development and use of mutation-targeted cancer therapies. Nat Biotechnol 2006;24:985–95.
25. Hicks DG, Tubbs RR. Assessment of the HER2 status in breast cancer by fluorescence *in situ* hybridization: a technical review with interpretive guidelines. Hum Pathol 2005;36:250–61.
26. Paik S, Bryant J, Tan-Chiu E, et al. Real-world performance of HER2 testing-National Surgical Adjuvant Breast and Bowel Project experience. J Natl Cancer Inst 2002;94:852–4.
27. Perez EA, Suman VJ, Davidson NE, et al. HER2 testing by local, central, and reference laboratories in specimens from the North Central Cancer Treatment Group N9831 intergroup adjuvant trial. J Clin Oncol 2006;24:3032–8.
28. Press MF, Sauter G, Bernstein L, et al. Diagnostic evaluation of HER-2 as a molecular target: an assessment of accuracy and reproducibility of laboratory testing in large, prospective, randomized clinical trials. Clin Cancer Res 2005;11:6598–607.
29. Reddy JC, Reimann JD, Anderson SM, Klein PM. Concordance between central and local laboratory HER2 testing from a community-based clinical study. Clin Breast Cancer 2006;7:153–7.
30. Roche PC, Suman VJ, Jenkins RB, et al. Concordance between local and central laboratory HER2 testing in the breast intergroup trial N9831. J Natl Cancer Inst 2002;94:855–7.
31. Wolff AC, Hammond ME, Schwartz JN, et al. American Society of Clinical Oncology/College of American Pathologists guideline recommendations for human epidermal growth factor receptor 2 testing in breast cancer. J Clin Oncol 2007;25:118–45.
32. Baker K, Randall M, Patel A, et al. Rapid monitoring of recombinant protein products: A comparison of current technologies. Trends Biotechnol 2002;20:149–56.